Rev. Roum. Sci. Techn.– Électrotechn. et Énerg.
Vol. **70**, *1*, pp. 145–150, Bucarest, 2025

ENERGY-BASED MODEL OF A LIQUID PISTON GAS COMPRESSION SYSTEM

OLEKSIY KUZNYETSOV [1,2], VITALII ATAMANIUK [2]

Keywords: Compressed air energy storage; Liquid piston; Port Hamiltonian system; Bond graph; Hydropneumatic accumulator; Energy-based model.

Compressed air energy storages (CAES) are used in autonomous or semi-autonomous renewable energy systems due to their advantages over battery energy storage, *e.g.*, environmental-friendly production process and sufficiently large number of cycles. Liquid piston (LP) technology for CAES is an alternative to other gas compression technologies developed to provide better heat transfer and thus increase energy efficiency. An energy-based model of a hydropneumatic accumulator using the LP gas compression in a port-Hamiltonian (pH) form is developed for control design. The bond graph framework is utilized to directly derive the equations in the pH form by exploiting the nonlinear fluid capacitance as a storage model. Nonlinearity is depicted analytically for a generalized polytropic process considering the ideal gas condition. The operation of the developed model is validated using MATLAB R2021b Simscape simulations.

1. INTRODUCTION

Future energy systems will increasingly rely on small-scale on-site local generation from renewable resources and autonomous and semiautonomous components. Energy storage is an integral part of these systems, compensating for irregularities and peak demand in energy generation and consumption. Compressed gas storage is an interesting option for mechanical energy storage due to its eco-friendly production and operation, safety issues, and a potentially unlimited number of cycles [1].

Compressed air energy storage (CAES) technology is well-suited to combining renewable resources such as wind, solar, or biomass [2]. A study [3] demonstrated the economic expediency of using CAES in urban conditions. This type of energy storage is also efficient in in-vehicle applications [4].

A type of hydropneumatic energy storage where gas is compressed by liquid piston (LP) technology [5] is proposed in [6] and provides several advantages over the traditional piston technology, including higher energy efficiency and better heat transfer. This technology is being increasingly developed, resulting in new LP designs with improved characteristics [7]. Its applications are in vehicle technology [4], wind [8], wave [9], energy conversion systems, *etc*.

From the control point of view, CAES is a nonlinear system that requires applying nonlinear control strategies. In the current study, we propose applying energy-based techniques to derive the mathematical model of the LP CAES system that can be used for control purposes.

The basic idea of the energy-based techniques is that the same approaches can be applied to describe the energy conversion, storage, and dissipation for objects of different physical nature. This study uses bond-graph and port-Hamiltonian frameworks to develop the model. Thus, bond graphs (BG) are historically the first developed energy-based technique from the pre-computer era; it is a powerful technique that can assist in deriving system equations and depicting the features of energy exchange, finding algebraic loops in the calculation, etc. [10,11]. BG can be easily converted to a common control engineering block diagram representation to proceed with the control design. On the other hand, due to its energy orientation, it can be used to switch to other energy-based frameworks, *e.g.*, the port-Hamiltonian (pH) one.

The latter is one of the energy-based approaches to modeling, analyzing, and controlling multidisciplinary systems [12]. Originally from mechanical engineering, this framework was later extended to multidisciplinary systems, allowing the development of control algorithms with intrinsic stability properties. Unlike the more traditional control engineering signal-based approach dealing with complex nonlinear systems, which is also the case for fuzzy logic [13,14], sliding mode control [15,16], optimization techniques [17–19], *etc*., energy-based control techniques are formulated from the point of view of the energy exchange between the components and therefore have a direct physical interpretation [20].

The article is organized as follows: first, we introduce the system under study, LP gas compression using an electric motor driving a pump; then, we briefly introduce the two energy-based frameworks, BG and pH; after that, we formulate the system model using the energy-based paradigm with BG as the basis to derive the pH equations; and finally, we validate the model using the MATLAB R2021b Simscape environment.

2. DESCRIPTION OF THE STUDIED SYSTEM

A system based on LP gas compression in a hydropneumatic accumulator was considered, i.e., a compression by an incoming liquid flow (Fig. 1). The liquid is pumped from a reservoir to an accumulator by a pump, producing a pressure difference Δp. At each time instance, accumulator volume V_{acc} consists of the volume of liquid V_{l} and the volume of gas V_{g}. The pressure of the gas inside the accumulator is p_2. The pump is fed by a DC motor M that generates torque τ to rotate the pump at the angular speed ω.

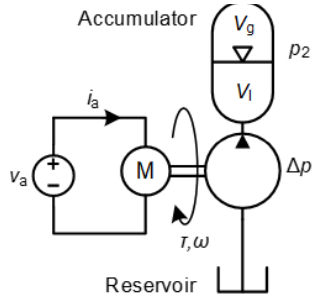

Fig. 1 – The studied liquid piston gas compression system.

[1] Institute of Power Engineering and Control Systems, Lviv Polytechnic National University, 12 S. Bandera Str., Lviv, 79013, Ukraine
[2] Department of Electromechanics and Electronics, Hetman Petro Sahaidachnyi National Army Academy, 32 Heroiv Maidanu Str., Lviv, 79026, Ukraine
E-mail: oleksii.o.kuznietsov@lpnu.ua, atamanvitalv@gmail.com

DOI: 10.59277/RRST-EE.2025.1.25

The motor is fed by a DC voltage source v_a with the current i_a flowing through the motor's armature circuit.

Below, we will derive a model of the system in Fig. 1 based on energy principles within the bond graph and the port-Hamiltonian frameworks.

3. PORT-HAMILTONIAN (PH) FRAMEWORK FOR ENERGY-BASED MODELLING

The Port-Hamiltonian (pH) framework is a unified multiphysical framework for the modeling, analysis and control of a wide class of nonlinear multidisciplinary systems [12].

The theory behind the framework originates from mechanical engineering, but it was later extended to any physical domain utilizing the notion of generalized displacements q and momenta p and focusing on energy exchange through the ports. The general mathematical formulation of a port-Hamiltonian system is as follows:

$$\begin{aligned} \dot{\mathbf{x}} &= \big(\mathbf{J}(\mathbf{x}) - \mathbf{R}(\mathbf{x})\big)\nabla H(\mathbf{x}) + \mathbf{G}(\mathbf{x})\mathbf{u}, \\ \mathbf{y} &= \mathbf{G}(\mathbf{x})^{\mathrm{T}}\nabla H(\mathbf{x}), \end{aligned} \tag{1}$$

where $\mathbf{x}(t) \in \mathrm{R}^n$ is the state vector containing generalized displacements and momenta, $H = \frac{1}{2}\mathbf{x}^{\mathrm{T}}\mathbf{D}^{-1}(\mathbf{x})\mathbf{x}$ is the Hamiltonian (total energy) function, $\mathbf{D}(\mathbf{x})$ is the diagonal matrix of inertia, $\mathbf{J}(\mathbf{x}) \in \mathrm{R}^{n\times n}$ is the skew-symmetric ($\mathbf{J}(\mathbf{x}) = -\mathbf{J}(\mathbf{x})$) matrix of interconnections, $\mathbf{R}(\mathbf{x}) \in \mathrm{R}^{n\times n}$ is the symmetric positive ($\mathbf{R}(\mathbf{x}) = \mathbf{R}(\mathbf{x})^{\mathrm{T}} \geqslant 0$) damping matrix, $\mathbf{G}(\mathbf{x}) \in \mathrm{R}^n$ is the input port matrix and $\mathbf{u}(t) \in \mathrm{R}^n$ is the vector of input energy variables.

4. BOND GRAPH FRAMEWORK

Bond graphs are the graphical energy-based framework used to define the relations between components that interact by exchanging energy [10]. It is a graphical approach that allows for a visual interpretation of the energy exchange between the energy ports using the bonds. It is based on the energy variables, generalized efforts e and generalized flows f, and the product of those in each domain (mechanical, electrical, etc.) is power. Generalized efforts and flows are related to generalized displacements and momenta as $\dot{q} = f$, and $\dot{p} = e$. In the current work, we use the notation where an effort variable is placed above the half-arrow of a bond and a flow one, below it.

The relations between the effort and flow variables are depicted by 0- and 1-junctions (Fig. 2 contains only the 1-junctions), so that for a 0-junction, efforts for all bonds are equal, and the sum of all flows is zero (accounting for input and output directions), and for a 1-junction, the flows are equal and the sum of all efforts is zero.

The energy elements used to depict the energy relations in the BG framework are the sources of effort **Se** and flow **Sf**, resistor **R**, inertia **I** and compliance **C**. The effort-flow relations for the latter three elements are defined as follows:

$$\mathbf{R}\colon e = Rf, \quad \mathbf{I}\colon \begin{cases} f = p/I \\ \dot{p} = e \end{cases}, \quad \mathbf{C}\colon \begin{cases} e = q/C, \\ \dot{q} = f, \end{cases} \tag{2}$$

where R, C, and I are the generalized resistance, compliance and inertia, respectively. As long as the equations of the energy storage elements in (2) contain $\dot{p}$ and $\dot{q}$, and the corresponding co-variables ($\frac{\partial H}{\partial p}$ and $\frac{\partial H}{\partial q}$, respectively), the relations defined by the bond graphs can be used to directly derive the first equation in (1).

The energy transformation is depicted by the transformer **TF** and the gyrator **GY** elements. In particular, for the pair of input (e_1, f_1) and output (e_2, f_2) variables the following relations hold for some ratios k_{TR} and k_{GY}, respectively:

$$\mathbf{TF}\colon \begin{cases} f_1 k_{\mathrm{TR}} = f_2 \\ e_2 k_{\mathrm{TR}} = e_1 \end{cases}, \quad \mathbf{GY}\colon \begin{cases} f_1 k_{\mathrm{GY}} = e_2 \\ f_2 k_{\mathrm{GY}} = e_1. \end{cases} \tag{3}$$

5. DERIVATION OF THE MATHEMATICAL MODEL FROM THE BOND GRAPH

5.1. BOND-GRAPH REPRESENTATION

The relations between the components of the system are described by the bond graph (Fig. 2) that contains electrical, mechanical, and hydraulic domains. The model accounts for the dissipation of the power in the **R** elements, energy storage in the **I** and **C** elements, and energy transformation, by the **TF** and **GY** elements.

The generalized efforts and flows for the domains are: voltage v and current i (electrical), torque and rotational speed ω (rotational mechanical), pressure p and flow rate $\dot{V}$ (hydraulic), respectively. The generalized displacements and momenta for the studied domains are: charge q and flux linkage λ (electrical), angle θ and angular momentum L (rotational mechanical), hydraulic momentum Γ and volume V (hydraulic), respectively.

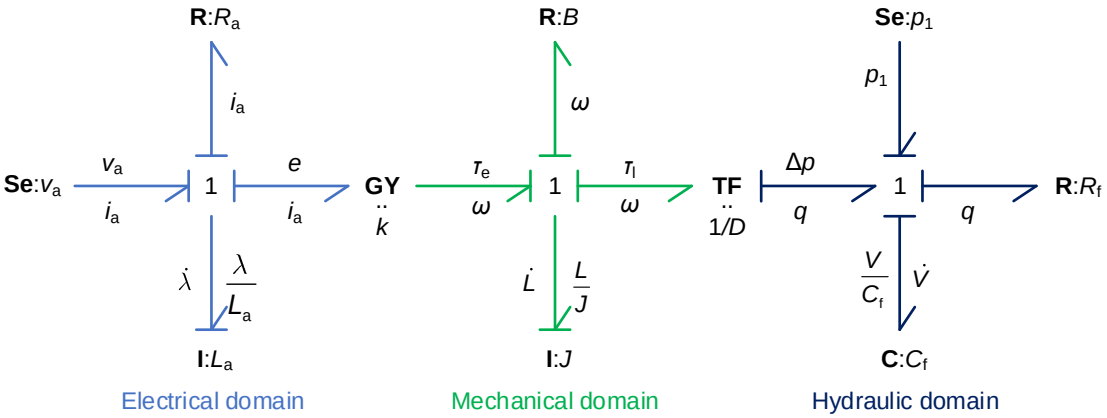

Fig. 2 – Bond graph model of a liquid piston gas compression system.

5.2. ELECTRICAL AND MECHANICAL DOMAINS

The electrical subsystem is modelled by a voltage source v_a represented in a BG by a source of effort **Se**, and DC motor winding inductance L_a and resistance R_a represented by inertia **I** and resistance **R**, respectively. The mechanical part of the motor and load (pump) accounts for the mechanical rotational inertia J (inertia **I**) and friction, with the coefficient B (resistance **R**). Under the constant magnetic field conditions, there is a proportional relation between the counter-e. m. f. of the winding and the rotational speed and between the torque and current with a coefficient k. That connection between the electrical and mechanical domains is modeled by a gyrator **GY** element that describes the relationship between efforts of one domain and flows of the other.

5.3. PUMP AND HYDRAULIC DOMAIN

The pump model takes into account the proportional relation between the torque of the pump shaft and a pressure difference Δp and between the rotational speed and volume flow q with the proportionality coefficient being the pump displacement D. The relation between the mechanical and the hydraulic domains is therefore between the corresponding efforts and between the corresponding flows, which is modeled by a transformer **TF** element.

Hydraulic subsystem models liquid movement from a reservoir to an accumulator. The pressure of a reservoir is represented by a source of effort **Se**; the fluid resistance of the penstock R_f, represented by a resistance **R** element, and an accumulator fluid capacitance C_f, by a compliance **C** element.

Fluid resistance models a relationship between the pressure p and a flow rate $\dot{V}$ as $p = R_f\dot{V}$. It can be obtained from the Poiseulle law as [21, pp. 223 – 224].

$$R_f = \frac{8\pi\mu l}{A_p^2},$$

where μ is dynamic water viscosity, l is the pipe length and A_p is the cross-section area of the pipe.

5.4. FLUID CAPACITANCE OF A COMPRESSED AIR STORAGE

For the hydropneumatic accumulator (Fig. 1), the relation between pressure and liquid flow rate is defined by the value of fluid capacitance C_f as

$$q = \frac{dV_l}{dt} = C_f\frac{dp}{dt}.$$

For a nonlinear relationship, it is useful to utilize the form of fluid capacitance as $C_f = V_l/p$ [21].

For CAES, the most effective mode of gas compression is isothermal [22] (pp. 151–160), however, a generalized polytropic gas compression should be considered. It is depicted by

$$pV_g^\gamma = \text{const.}, \tag{4}$$

where γ is the polytropic constant.

Consider a gas compression by means of LP (Fig. 1) from the initial state characterized by the pressure p_{init} and volume equal to V_{acc} to the final one with pressure p and volume V_g. Writing eq. (4) for the two states, we obtain the following:

$$p_{init}V_{acc}^\gamma = pV_g^\gamma = p(V_{acc} - V_l)^\gamma. \tag{5}$$

From (5), the pressure is obtained as

$$p = \frac{p_{init}V_{acc}^\gamma}{(V_{acc} - V_l)^\gamma} \tag{6}$$

and the fluid capacitance is, therefore,

$$C_f = \frac{V_l}{p} = \frac{V_l(V_{acc} - V_l)^\gamma}{p_{init}V_{acc}^\gamma}. \tag{7}$$

To analyze the nonlinear behavior of the fluid capacitance of the LP, eq. (7) can be written in a dimensionless per-unit form by introducing the variables $V_l^* = V_l/V_{acc}$ $(0 \le V_l^* < 1)$ and $C_f^* = C_f p_{init}/V_{acc}$. Thus, eq. (7) is transformed into the form

$$C_f^*(V_l^*) = V_l^*(1 - V_l^*)^\gamma, \tag{8}$$

suitable for the analysis of the dependence of dimensionless fluid capacitance on the dimensionless liquid volume inside the accumulator. The dependence (8) is represented in Fig. 3 for polytropic constants from isothermal (γ = 1) to adiabatic (γ = 1.4) cases.

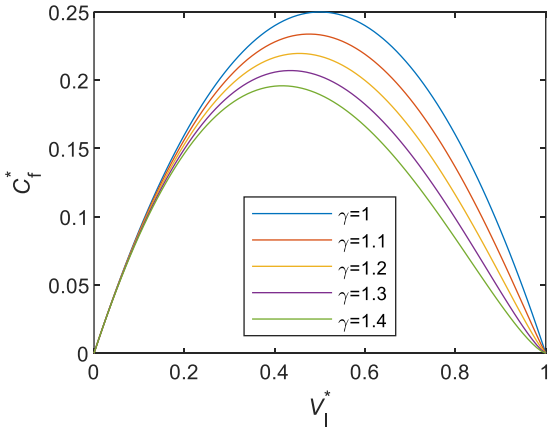

Fig. 3 – Nonlinear dependence of dimensionless fluid capacitance $C_f^*(V_l^*)$ for different polytropic constants γ.

5.5. PORT-HAMILTONIAN REPRESENTATION

Based on the bond graph model (Fig. 2), the state variables vector with the components associated with the energy storage components is

$$\mathbf{x} = (\lambda \quad L \quad V)^\top = (L_a i \quad J\omega \quad C_f p)^\top.$$

These generalized momenta of the inertia components and generalized displacents of a compliance component (so that efforts and flows explicitly contain the time derivatives of the elements of the state vector **x**).

Based on a BG in Fig. 2,

$$\dot{\lambda} = v_a - R_a\left(\frac{\lambda}{L_a}\right) - k\left(\frac{L}{J}\right),\ \dot{L} = k\left(\frac{\lambda}{L_a}\right) - B\left(\frac{L}{J}\right) - D\Delta p,\ \dot{V} = D\left(\frac{L}{J}\right). \tag{9}$$

For a detailed explanation of the derivation of the equations from the BG, the authors refer the reader to [10,11]. In short, we are following the effort or flow variable the relations dictated by the components and junctions as explained above. Thus, the first eq. (9) corresponds to the effort balance written for the left 1-junction taking into account the dependencies between the efforts and the flows for the surrounding components. Likewise, the relation for the pressure difference is derived from the same diagram as

$$\Delta p = R_f D\left(\frac{L}{J}\right) + \left(\frac{V}{C_f}\right) - p_1.$$

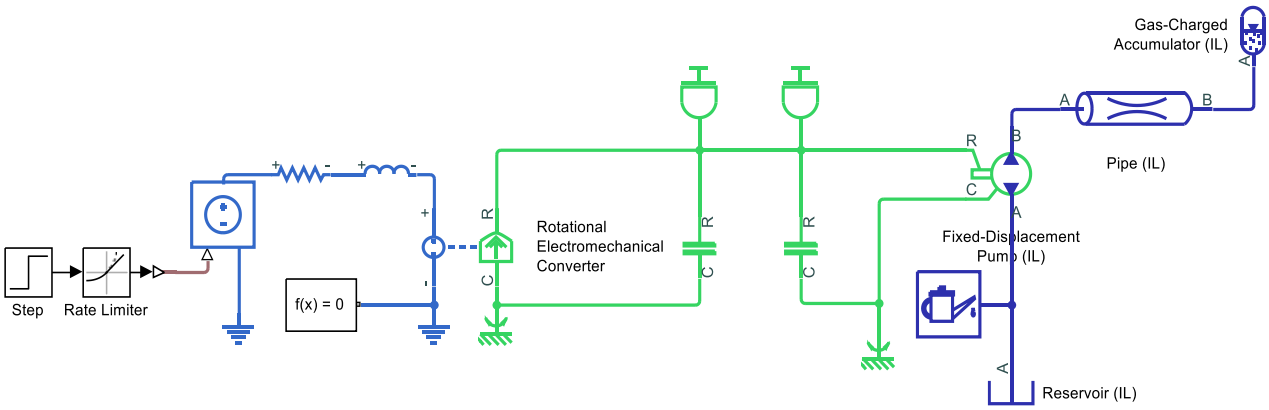

Fig.4 – Simscape model of the LP CAES system.

By collecting similar terms in (9), we obtain

$$\dot{\lambda} = v_a - R_a\left(\frac{\lambda}{L_a}\right) - k\left(\frac{L}{J}\right),$$

$$\dot{L} = k\left(\frac{\lambda}{L_a}\right) - \left(B + R_f D^2\right)\left(\frac{L}{J}\right) - D\left(\frac{V}{C_f}\right) + Dp_1, \qquad (10)$$

$$\dot{V} = D\left(\frac{L}{J}\right).$$

The model (10) can be easily represented in a pH form (1). First, a Hamiltonian (a full-energy) function is formulated:

$$H(\mathbf{x}) = \frac{1}{2}\left(L_a i_a^2 + J\omega^2 + C_f p^2\right) = \frac{1}{2}\left(\frac{\lambda^2}{L_a} + \frac{L^2}{J} + \frac{V^2}{C_f}\right)$$

and the vector of covariables as

$$\nabla H(\mathbf{x}) = \left(\frac{\partial H}{\partial \lambda} \quad \frac{\partial H}{\partial L} \quad \frac{\partial H}{\partial V}\right)^{\mathrm{T}} = (i_a \ \omega \ p)^{\mathrm{T}} = \left(\frac{\lambda}{L_a} \quad \frac{L}{J} \quad \frac{V}{C_f}\right)^{\mathrm{T}}.$$

The matrices and vectors in a *p-H* representation (1) are defined as follows:

$\mathbf{J}(\mathbf{x}) = \begin{pmatrix} 0 & -k & 0 \\ k & 0 & -D \\ 0 & D & 0 \end{pmatrix}$, $\mathbf{G}(\mathbf{x}) = \mathbf{I}_3$, where $\mathbf{I}_3$ is 3×3 identity matrix,

$\mathbf{R}(\mathbf{x}) = \mathrm{diag}(R_a \quad B + R_f D^2 \quad 0)$, $\mathbf{y} = (i_a \quad \omega \quad p)^{\mathrm{T}}$,

$\mathbf{u} = (v_a \quad Dp_1 \quad 0)^{\mathrm{T}}$, $D = \mathrm{diag}(L_a \quad J \quad C_f)$.

The derived LP CAES model in the form (1) with all matrices being defined as explained above has been implemented as a MATLAB script using the ode45 function is for numerical integration. A new fluid capacitance value is obtained at each time step using the relation $C_f = V/p$.

6. VALIDATION OF THE ENERGY-BASED MODEL

The computer model of the LP CAES (Fig. 1) has been developed using the Simscape package (MATLAB version R2021b, Fig. 4). The model contains three domains, electrical (light blue), mechanical (light green), and isothermal liquid (dark blue). The electrical subsystem contains the voltage source controlled by the step signal passing through the rate limiter to limit the starting current, *RL* link for the parameters of the motor winding and a *Rotational Electromechanical Converter* block connecting the electrical and the mechanical subsystems.

The mechanical parts of the motor and pump are implemented using the *Inertia* and *Rotational Friction* blocks. It should be noted that the Simscape library also contains a *DC Motor* block, but it allows no access to the motor's electrical torque, while its computational implementation is the same. The *Fixed-Displacement Pump (IL)* block connects the mechanical and isothermal liquid domain. In the latter, the water is pumped from the reservoir through the pipe to the LP CAES implemented as the *Gas-Charged Accumulator (IL)* block. The simulation results obtained from the Simscape model are transferred to the MATLAB Workspace using the Simscape Results Explorer tool to compare the obtained MATLAB Workspace variables with those from the pH-based model.

First, the compression process for isothermal conditions (for $\gamma = 1$) and adiabatic conditions (for $\gamma = 1.4$) was compared. A collection of waveforms corresponding to those cases is provided in Fig. 5 and Fig. 6, with only a slight difference between the results obtained by the two models.

When a simulation is performed for up to the full filling of the container, a longer simulation is performed (Fig. 7). Therefore, the fluid capacitance value (calculated for both cases as $C_f = V/p$) modeling of the behavior of hydropneumatic accumulator changes over an almost complete range (Fig. 8).

Although the processes in the electrical and mechanical domains are quite similar, in the hydraulic domain, the difference between the results of the pressure curve is larger. The fluid capacitances for both cases are quite similar, therefore, the source of the difference in behavior is the pump. Indeed, while the pH model represents the pump without taking into account the pressure losses and the volumetric losses, those are implemented in the Simscape model and are quite close to the real behavior of the pump. Insofar as the proposed pH model is developed for control system design, not for simulation studies, we assume that the accuracy of the model is adequate for the control system design, which is the direction of our future studies.

Otherwise, the more complex pump models can be developed, *e.g.*, using the bond-graph models proposed in [23] or [24]. The other direction of future research is the formulation of an LP CAES in the form of irreversible pH systems considering the process's thermodynamics [25,26].

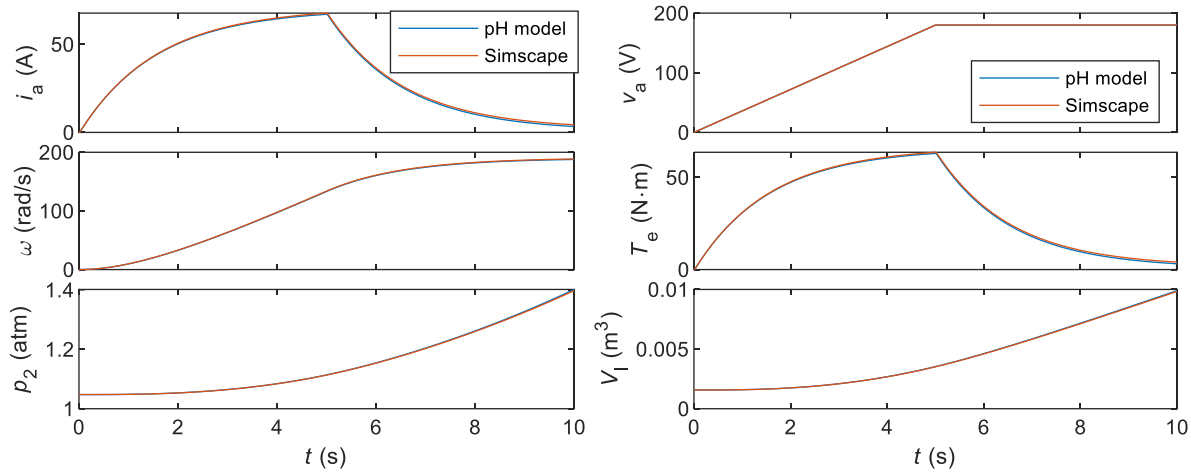

Fig. 5 – Model validation, isothermal process ($\gamma = 1$).

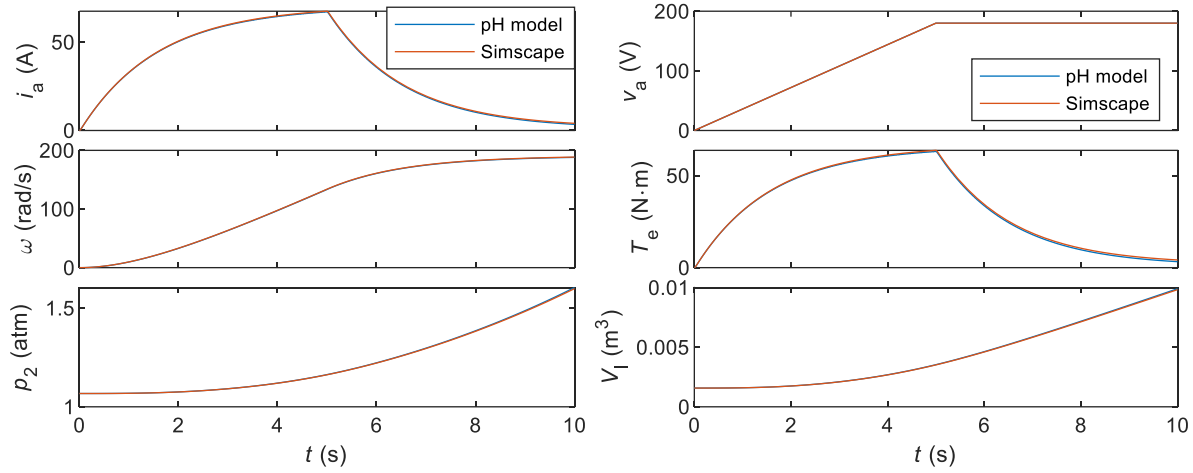

Fig. 6 – Model validation, adiabatic process ($\gamma = 1.4$).

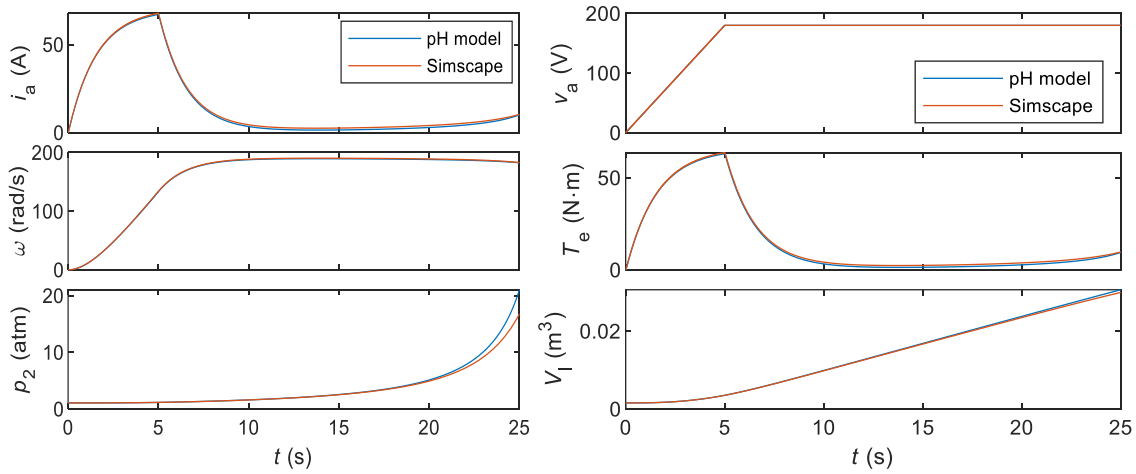

Fig. 7 – Model validation for the full filling of the container.

7. **CONCLUSIONS**

This paper presents an energy-based liquid piston compressed air energy storage system model in a port Hamiltonian formulation. This representation can be simple enough to be used in the control synthesis, and the nonlinearity of fluid capacitance captures the nonlinear behavior of the hydropneumatic accumulator. The latter is formulated analytically for a generalized polytropic compression. Such a representation is inspired by the bond graph framework, and in the current study, we exploited the possibility of using bond graphs to directly formulate the mathematical model in a form suitable for port-Hamiltonian representation.

The developed energy-based pH model is implemented as a Matlab script and validated utilizing the Simscape model.

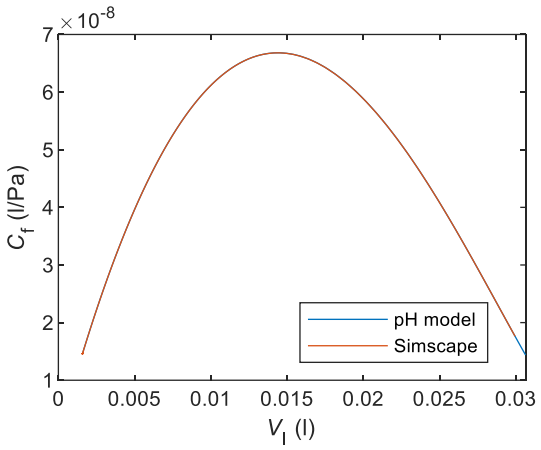

Fig. 8 – Comparing the fluid capacitance values for both models.

The directions of future research are formulated as follows: first, study the control system with a proposed port-Hamiltonian model; if the behavior is unsatisfactory, (i) try to use a more complex pump model, and (ii) try to use the formulation in terms of irreversible port-Hamiltonian systems.

APPENDIX. PARAMETERS OF THE SYSTEM

DC motor: input voltage $v_a = 180$ V, nominal power $P_n = 1.5$ kW, efficiency $\eta = 0.87$, armature resistance $R_a = 0.8093$ Ω, armature inductance $L_a = 11.508$ mH; inertia $J_m = 1.7048$ N·m·s^2; viscous damping $B_m = 0$.

Pump: displacement $D = 46$ cm^3/rev; nominal shaft angular velocity $\omega_n = 157$ rad/s; nominal pressure gains $\Delta p = 10$ atm; volumetric efficiency $\eta_v = 0.92$; mechanical efficiency $\eta_m = 0.88$; inertia $J_p = 2.5$ mN·m·s^2; viscous damping $B_p = 2.03$ mN·s/m.

Penstock: length $l_p = 1$ m, diameter $d_p = 0.01$ m.

Hydropneumatic accumulator: length $l_{acc} = 1.1$ m; diameter $d_{acc} = 0.2$ m.

Received on 14 October 2024

CREDIT AUTHORSHIP CONTRIBUTION

Oleksiy Kuznyetsov: Conceptualization, methodology, software, Validation, formal analysis, investigation, writing – original draft, writing – review & editing, visualization, supervision.

Vitalii Atamaniuk: Validation, formal analysis, investigation, writing – review & editing.

REFERENCES

1. R.A. Rabi, J. Radulovic, J. Buick, *Comprehensive review of compressed air energy storage (CAES) technologies*, Thermo., **3**, *1*, pp. 104–126 (2023).
2. H. Guo, H. Kang, Y. Xu, M. Zhao, Y. Zhu, H. Zhang, H. Chen, *Review of coupling methods of compressed air energy storage systems and renewable energy resources*, Energies, **16**, *12*, 4667 (2023).
3. E. Bazdar, F. Nasiri, F. Haghighat, *Optimal planning and configuration of adiabatic-compressed air energy storage for urban buildings application: Techno-economic and environmental assessment*, J. Energy Storage, **76**, 109720 (2024).
4. H. Tian, H. Zhang, Z. Yin, Y. Liu, X. Zhang, Y. Xu, H. Chen, *Advancements in compressed air engine technology and power system integration: A comprehensive review*, Energy Rev., **2**, *4*, 100050 (2023).
5. J.D. van de Ven, P.Y. Li, *Liquid piston gas compression*, Appl. Energy, **86**, *10*, pp. 2183–2191 (2009).
6. R. Lemofouet, A. Rufer, *A hybrid energy storage system based on compressed air and supercapacitors with maximum efficiency point tracking (MEPT)*, IEEE Trans. Ind. Electron., **53**, *4*, pp. 1105–1115 (2006).
7. E.M. Gouda, Y. Fan, M. Benaouicha, T. Neu, L. Luo, *Review on liquid piston technology for compressed air energy storage*, Sci. World J., **2014**, 289839 (2014).
8. M. Saadat, P.Y. Li, T.W. Simon, *Optimal trajectories for a liquid piston compressor/expander in a compressed air energy storage system with consideration of heat transfer and friction*, Am. Control Conf. (ACC), pp. 1800–1805, 2012.
9. S. Ma, X. Wang, M. Negnevitsky, E. Franklin, *Performance investigation of a wave-driven compressed air energy storage system*, J. Energy Storage, **73**, 109126 (2023).
10. P.J. Gawthorp, G.P. Bevant, *Bond-graph modeling*, IEEE Control Syst., **27**, *2*, pp. 24–45 (2007).
11. W. Borutzky, *Bond graph modelling and simulation of multidisciplinary systems – An introduction*, Simul. Model. Pract. Theory, **17**, *1*, pp. 3–21 (2009).
12. A. van der Schaft, *Port-Hamiltonian modeling for control*, Annu. Rev. Control Robot. Auton. Syst., **3**, *1*, pp. 393–416 (2020).
13. S. Mahdab, A. Moualdia, *Intelligent management of a hybrid system by fuzzy logic: application to arc welding*, Rev. Roum. Sci. Techn. – Électrotechn. et Énerg., **67**, *2*, pp. 111–116 (2022).
14. Widjonarko, S.R. Soenoko, S. Wahyudi, E. Siswanto, *Design of air motor speed control system for small scale compressed air energy storage using fuzzy logic*, IOP Conf. Ser.: Mater. Sci. Eng., **494**, 012025 (2019).
15. Y. Oubbati, B.K. Oubbati, A. Rabhi, S. Arif, *Experimental analysis of hybrid energy storage system based on nonlinear control strategy*, Rev. Roum. Sci. Techn. – Électrotechn. et Énerg., **68**, *1*, pp. 96–101 (2023).
16. G. Tu, Y. Li, J. Xiang, *Sliding mode control of energy storage systems for reshaping the accelerating power of synchronous generators*, IEEE Trans. Power Syst., **38**, *2*, pp. 1242–1256 (2023).
17. K. Venugopalan, J. Varghese, J. Thankaswamy, *African vulture optimized integrated control technique for PV-fed open-end winding induction motor pump application*, Rev. Roum. Sci. Techn. – Électrotechn. et Énerg., **69**, *1*, pp. 27–32 (2024).
18. X. Huang, R. Hao, L. Zhang, H. Sun, Q. Zheng, *System modeling and compression efficiency optimal control of hydro-pneumatic cycling compressed air energy storage system*, Zhongguo Dianji Gongcheng Xuebao/Proc. Chin. Soc. Electr. Eng., **34**, *13*, pp. 2047–2054 (2014).
19. J. Bai, W. Wei, S. Mei, *Optimal charging power tracking control of advanced adiabatic compressed air energy storage over wide operation ranges*, 6th Int. Conf. Smart Grid Smart Cities (ICSGSC), pp. 24–32, Chengdu, China, 2022.
20. R. Ortega, A.J. van der Schaft, I. Mareels, B. Maschke, *Putting energy back in control*, IEEE Control Syst. Mag., **21**, *2*, pp. 118–33 (2001).
21. B.T. Kulakowski, F. Gardner, J.L. Shearer, *Dynamic Modeling and Control of Engineering Systems* (3rd ed.), Cambridge University Press, 2007, pp. 219–224.
22. A. Rufer, *Energy Storage: Systems and Components* (1st ed.), CRC Press, 2017, pp.151–160.
23. R. Ramakrishnan, S.S. Hiremath, M. Singaperumal, *Dynamic analysis and design optimization of series hydraulic hybrid system through power bond graph approach*, Int. J. Vehicular Technol., **2014**, pp. 1–19 (2014).
24. Y. Li, Z. Zhu, G. Chen, *Bond graph modeling and validation of an energy regenerative system for emulsion pump tests*, Sci. World J., **2014**, 289839 (2014).
25. A. van der Schaft, *Geometric modeling for control of thermodynamic systems*, Entropy, **25**, *4*, 577 (2023).
26. H. Ramirez, Y. le Gorrec, *An overview on irreversible port-Hamiltonian systems*, Entropy, **24**, *10*, 1478 (2022).